Identifying Pathfinder Elements of Gold in the Wa-Lawra Belt, NW Ghana: Constraints from Petrography, Multi-Element Geochemistry, and Multivariate Statistical Analysis

[1,2*]Emmanuel Daanoba Sunkari, [1]Samuel Edem Kodzo Tetteh, [3]Moses Sumbobo & [4]Yılmaz Demir

[1]Department of Geological Engineering, Faculty of Geosciences and Environmental Studies, University of Mines and Technology, P.O. Box 237, Tarkwa, Ghana

[2]Department of Geological Engineering, Faculty of Engineering, Niğde Ömer Halisdemir University, 51240, Main Campus, Niğde, Turkey

[3]Azumah Resources Ghana Limited, P.O. Box ND 24, Nadowli, Upper West Region, Ghana

[4]Department of Geological Engineering, Recep Tayyip Erdoğan University, 53100, Rize, Turkey

*Corresponding Author: edsunkari@umat.edu.gh

Sunkari, E.D., **Tetteh, S.E.K**., Sumbobo, M. and Demir. Y. (2022). Identifying pathfinder elements of gold in the Wa-Lawra Belt, NW Ghana: Constraints from petrography, multi-element geochemistry, and multivariate statistical analysis. In 7*th UMaT Biennial International Mining and Mineral Conference*, Tarkwa,Ghana, pp. 1-13.

Abstract

The Wa-Lawra greenstone belt is located in northwest Ghana and is largely dominated by Birimian metavolcanics, volcaniclastics, and metasediments. Previously, regolith materials such as laterites and soils from mixed sources were used to identify pathfinder elements of gold in the belt. However, in-situ laterites will better represent their underlying formations than transported laterites that may contain extraneous sources of element enrichment caused by pollution, which is unrelated to gold mineralization. In this study, petrographic studies of residual laterites and statistical analyses of trace element geochemical data of the residual laterites were performed to identify the pathfinder elements of gold in the Wa-Lawra greenstone belt. Six fresh residual laterite samples were used for the petrographic studies, which revealed the dominance of quartz, amphibole, clinopyroxene, hematite, goethite, magnetite, sphalerite, and pyrite. These minerals contribute Fe, S, Ca, Zn, and other elements to the laterites. The geochemical data of 12 residual laterite samples were used for statistical analysis. P-P plots revealed deviations from the normal distribution and outliers in the dataset. Spearman's correlation revealed that Cu, Ag As, Pb, Fe, and S have a moderate-strong positive correlation with Au. Hierarchical cluster analysis revealed that there are 3 multi-element associations; a) Fe, Pb, Mn, S, Co, Au, Cr, Cu, Ni, Ag; b) Ti, Zr, Sr, Ca, and c) Rb, Y, Zn, As. Factor analysis shows that the occurrence of Pb, Cu, Ag, and As is directly related to the occurrence of Au. Thus, the best multi-element association of Au for exploration purposes is Pb, Cu, Ag, and As, similar to the previous findings. Single and multi-element anomaly mapping revealed that geochemical anomalies involving these elements are mainly found around the northern and southern parts of the study area. The results of this study confirm what has been reported by the previous studies.

Keywords: laterites, geochemical anomaly, gold, multivariate statistical analysis, petrography

1 Introduction

The Wa-Lawra Belt shows great promise for commercially viable gold mineralization, but several attempts in exploring and exploiting the resource have been largely unsuccessful over the years (Waller *et al.,* 2012). Sunkari *et al.* (2019) indicated that there is a contrast between the climatic conditions prevailing in northern and southern parts of the country. Savannah climate exists in northern Ghana, leading to a landscape that is a deeply weathered terrane with abundant laterites (Fig. 1). The landscape contrasts between the savannah and rainforest regions (Fig. 1) are a

result of changes to differences in climate, the nature of biological activities in both regions, topography variations, and the mode of lateritization (Arhin, 2013).

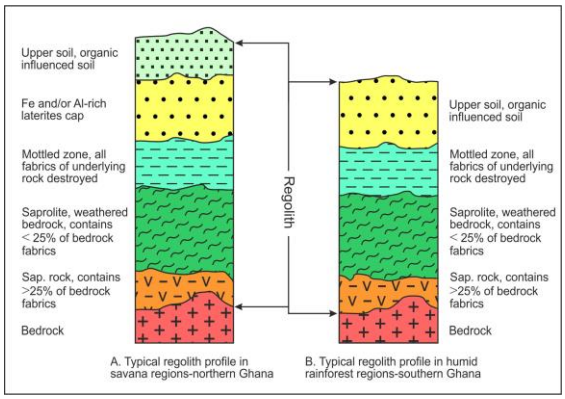

Figure 1. Typical regolith profiles in Savannah and rainforest regions of Ghana (after Arhin and Nude, 2009).

This implies that how elements are mobilized and/or dispersed by different geochemical processes in northern Ghana varies from that of southern Ghana and hence, different methods of mineral exploration, as well as different methods of interpretation of geochemical signature, are required in the Wa-Lawra Belt (Sunkari *et al*., 2019). Hence, several researchers used statistical methods to identify pathfinder elements of gold in the Wa-Lawra Belt. Nude *et al*. (2012) identified indicator elements for Au to be Pb, Ag, As, Cu, Fe, and Mn using soil samples from the Wa-Lawra Belt. Sunkari *et al*. (2019) also identified Pb, Cu, As, and Ag as indicator elements for Au using laterites from the Wa-Lawra Belt. These studies agree that laterites are the best geochemical sampling material in studies carried out purposefully to find the indicator elements of Au in deeply weathered regolith terranes, and the most useful pathfinder elements of Au in the area are As, Ag, Cu, and Pb. In both cases, both residual and transported laterites were used for the analysis.

The petrography of the laterites was also not studied. Generally, in-situ (residual) laterites will better represent their underlying formations than transported soils. Also, transported laterites may contain extraneous sources of element enrichment caused by pollution, which is unrelated to gold mineralization.

There is, therefore, a gap in the previous works done in the area. The gap this study seeks to fill is to determine the minerals associated with the laterites and the implications when only residual laterites are used for the analysis. This brings the following research questions to the forefront: Will the residual laterites be more effective in determining pathfinder elements of gold, or will similar results be obtained as before? What are the rock-forming minerals and ore minerals associated with the formation of the residual laterites? What will be the implications for gold exploration in the area? Therefore, this study aims to conduct petrographic studies, multi-element geochemical analysis, and multivariate statistical analysis of residual laterites in the Wa-Lawra Belt.

1.1 Geology of the Kunche Area

The Wa-Lawra greenstone belt is located in northwest Ghana (Fig. 2). This study is focused on the Kunche area in the Nadowli-Kaleo District of the Upper West Region in the Wa-Lawra greenstone belt (Fig. 2).

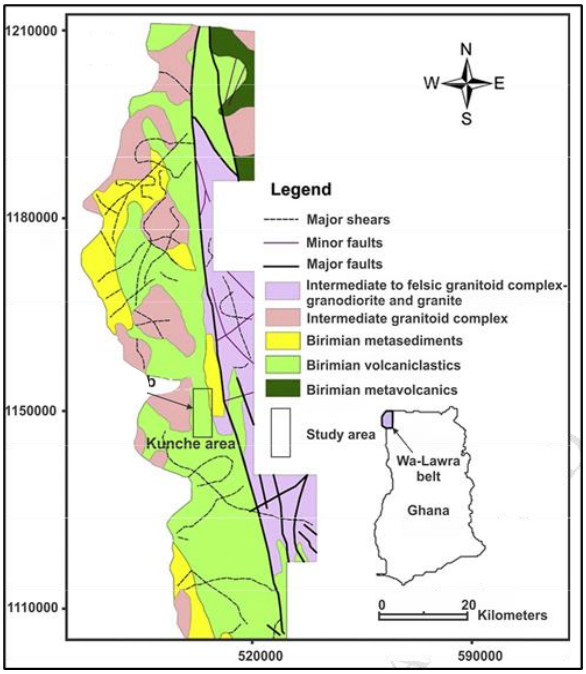

Figure 2. Geological map of the Wa-Lawra Belt showing the dominance of Birimian volcaniclastics in the Kunche area (after Arhin *et al.*, 2015)

The area is dominated by Birimian metavolcanic and volcaniclastics, Birimian metasediments, and some intrusive granitoids (Sunkari and Zango, 2018). Metamorphosed lavas and pyroclastic rocks,

namely basalts, andesite, rhyolites, and dolerites which are intruded in some places by gabbro are the major metavolcanic rocks in the area (Nude *et al*., 2012). The dominant metasedimentary rocks in the area include phyllite, sericite-schist, and meta-greywacke, which are intruded in some places by dykes of felsic and mafic nature (Arhin and Nude, 2009).

The Birimian Greenstone Belts found in Ghana host orogenic gold formed by hydrothermal fluids from metamorphism (Griffis *et al*., 2002). The mineralization is associated with mesothermal quartz veins found in both Upper and Lower Birimian rocks (Griffis *et al*., 2002). Amponsah *et al*. (2015) along with many other authors, acknowledged that the veins associated with Au mineralization are quartz veins where quartz has a dark gray color. The ore minerals which are associated with this mineralization style which are common in the area include pyrite, arsenopyrite, chalcopyrite, sphalerite, and galena while the associated gangue minerals include calcite, chlorite, ankerite, and tourmaline (Amponsah *et al*., 2015). Most rock units in the Kunche area host quartz veins, but those mineralized are usually seen to occur with sections of faulting and shearing found at contact zones between the Upper and Lower Birimian rock units (Nude *et al*., 2012). Waller *et al*. (2012) revealed that there is a shear zone known as the Kunche Shear Zone within which the quartz veins formed and that this Kunche Shear Zone contains interfused phyllites and greywackes, which have undergone intense brecciation due to the crustal shortening that deformed and disturbed the veins.

2 Materials and Methods Used

2.1 Sample collection and geochemical analysis

For this study, fresh residual laterite samples were obtained from the Kunche area, following the same protocols used by Sunkari *et al*. (2019) (Fig. 3). Fifteen samples were obtained from old pits and in-situ materials on the surface. Only 6 of these samples were used for petrographic analysis. Also, secondary laterite geochemical data were obtained from earlier research that studied the spatial distribution and the trace element geochemistry of laterites in the Kunche area, and their implication for gold exploration targets in NW Ghana as carried out by Sunkari *et al*. (2019). For this study, however, only the results of lateritic duricrust (residual laterite) samples, constituting 12 out of the 67 samples, were considered.

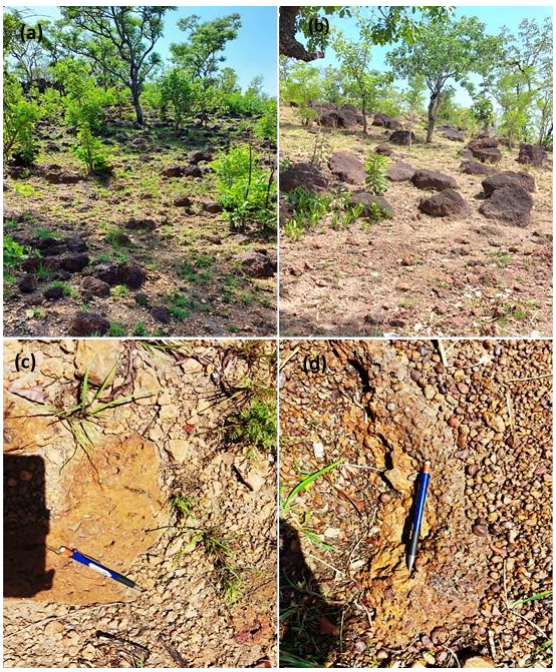

Figure 3. Photographs of lateritic duricrusts on hills in the Kunche area.

2.2 Petrographic analysis

Six samples (KL01, KL02, KL03, KL04, KL05, and KL06) were selected to prepare thin and polished sections. To identify the minerals and their associations within the residual laterites from the Kunche area, the thin and polished sections were studied under the microscope at the petrology laboratory of the Geological Engineering Department of the University of Mines and Technology (UMaT), Tarkwa.

2.3 Data processing and statistical methods

2.3.1 P-P plots

For a normally distributed dataset, the scatters on P-P plots should fall on or tightly close to the normal distribution line (Gao and Chik, 2013). For this study, P-P plots were used to check whether or not the data set is normally distributed before multivariate statistical analysis.

2.3.2 Spearman's correlation

Spearman's correlation

The relationship between any two variables in geochemistry can be determined taking into consideration the multivariate and regionalized character of the variables using the two-tailed Spearman's correlation method (Sunkari *et al*., 2019). Correlation is denoted by ***r*** where $-1 \leq r \leq 1$. The closer the value is to 1 or -1, the stronger the correlation. In many studies with several variables, the correlation between the variables is often computed in a tabular form as the correlation matrix (Debrah, 2013). That is, correlation is negligible between 0.00-0.30, low between 0.30-0.50, moderate for 0.50-0.70, high for 0.70-0.90, and very high between 0.90-1.00.

2.3.3 Centered log-ratio (CLR) transformation

Since geochemical data usually deviates from the normal, Centered Log-Ratio (CLR) Transformation was executed on the dataset to lower the gap that exists between the minimum and maximum contents within the multi-element dataset obtained from XRF and ICP-MS analysis (Zhao *et al*., 2015). The CLR is mathematically expressed as:

$$CLR(x) = \left(\log\left(\frac{x1}{g(x)}\right), \ldots, \log\left(\frac{xN}{g(x)}\right)\right) \ldots\ldots\ldots\ldots(1)$$

In the above formula, the contents for single elements in the samples are represented by $x1, x2 \ldots xN$, the variable x stands for the composition vector, and the geometric mean is given by g(x).

2.3.4 Hierarchical cluster analysis (HCA) and factor analysis

In analyzing the dataset obtained to identify relationships between gold and the elements as well as their possible sources, factor analysis with principal component analysis method as the extraction criterion and hierarchical cluster analysis (HCA) were used in the SPSS environment. The results of the HCA were presented using dendrograms. The dendrograms show the steps used by the software in obtaining the solution, the multi-element clusters, and the distances separating these multi-element clusters known as the squared Euclidean distance (Nude *et al*., 2012).

During the factor analysis, the principal component analysis method was applied in which principal components (factors) were obtained from the data, where each factor shows a certain process or groups of them responsible for how parameter values vary spatially (Sunkari et al., 2020). To obtain the number of components to extract, the Kaiser Criterion was used. The Kaiser Criterion extracts only principal components having eigenvalues of 1or more than 1. Scree plots show the number of components while the covariance matrix indicates the index of similarity (Nude *et al.*, 2012).

2.3.5 Delineation of geochemical anomalies

To separate anomaly from background values, anomaly thresholds were calculated such that those values that are more than the threshold are the anomalies of interest in geochemistry. Reimann *et al*. (2005) proposed a means of finding the anomaly threshold. This method was used for this study. If T represents the threshold value, med represents the median of a given element and MAD represents the median absolute deviation, and then the following formula is used;

$$T = med + 2MAD \ldots\ldots\ldots\ldots\ldots\ldots\ldots\ldots\ldots\ldots(2)$$

The median absolute deviation of a dataset represents the average distance between each data point and the mean and MAD gives an idea about the variability in a dataset, which is a measure of how dispersed the data is (Reimann *et al*., 2005). MAD is determined by the formula given that x_i represents the concentration of elements;

$$MAD = median\ |xi - median\ (xi)| \ldots\ldots\ldots\ldots(3)$$

MAD is instrumental in determining geochemical halos in a single element (Sunkari *et al.*, 2019). Dispersal patterns or signatures can better be defined by combining more than one indicator element when compared to the single element technique (Reis *et al*., 2001). This combination method is known as the multi-element halos technique. The multi-element halo technique was used together with the computed thresholds to determine geochemical halos associated with the existence of enriched pathfinder elements related to Au mineralization in the Kunche area. The formula used is given as;

$$H(X+Y) = \left(\frac{X_1}{X_0} + \frac{Y_1}{Y_0}\right); \left(\frac{X_2}{X_0} + \frac{Y_2}{Y_0}\right); \ldots; \left(\frac{X_N}{X_0} + \frac{Y_N}{Y_0}\right) (4)$$

X_1, X_2, …, X_N are concentrations of X in samples 1, 2, …, N. Y_1, Y_2, …, Y_N are concentrations of Y

in samples 1, 2, …, N. X_0 and Y_0 are threshold values of X and Y elements.

To generate maps that show single element and multi-element anomaly distributions, Geographic Information System (GIS) application software, ArcMap, version 10.8 was used. These maps were generated to understand spatial patterns.

Using Inverse Distance Weighting (IDW) Method, the single and multi-element threshold results aided in producing the geochemical anomaly map of the study area.

3 Results and Discussions

3.1 Petrography of the residual laterites

The microscopic studies of the residual laterites under transmitted light reveal a hypidiomorphic texture for many of the sections, dominated by subhedral-anhedral amphibole, clinopyroxene, quartz, and some opaque minerals (Fig. 4a-f).

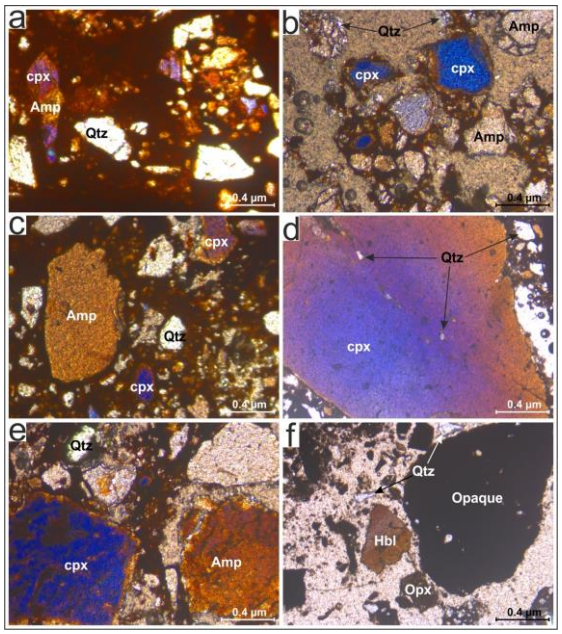

Figure 4. Photomicrograph Images of the Studied Samples Showing (Qtz = Quartz, Amp = Amphibole, Hbl = Hornblende, Cpx = Clinopyroxene, Opx = Orthopyroxene, Hem = Hematite, Gth = Goethite)

Due to the deformation in the samples, there are some shear zones observed along the crystal boundaries of amphiboles, which are generally filled with recrystallized quartz and late-stage clinopyroxenes that also overprint the amphiboles (Fig. 4b).

The weathering of amphiboles such as hornblende ($Ca_2(Mg, Fe)_4Al (Si, Al) O_{22}(OH, F)_2$)) contributes Ca and Fe contents to the laterites as well as stable phases of late-stage quartz. Similarly, clinopyroxenes present such as diopside ($MgCaSi_2O_6$) and orthopyroxene in the form of ferrosilite ($Fe_2Si_2O_6$) breakdown chemically invariably into quartz, releasing Ca and Fe during lateritization. This observation is corroborated by a similar observation made by Akintola *et al*. (2013) that hornblende is the major source of Fe and Ca and some trace elements in the regolith. Thus, the relatively high Fe and Mg contents may be explained in part as being input from weathering of mafic rocks and high-temperature minerals in the Kunche area. Magnetite (Fe_3O_4) and hematite (Fe_2O_3) in the laterites, which both crystallize in an environment with moderate oxygen levels, were originally formed via magmatic crystallization in the now metamorphosed igneous rocks and by hydrothermal fluid action within the metamorphic rocks (Reid, 2019). The rocks from which the laterites were formed in the Kunche area are no exceptions. Magnetite and hematite are persistent within the laterites due to their moderate resistance to weathering.

Microscopic studies under reflected light show hematite, magnetite, goethite, pyrite, and sphalerite as the dominant minerals within the residual laterites (Fig. 5a-f). Selvages and blebs of sphalerite appear to grow within masses of hematite (Fig. 5a), whereas magnetite masses with a grey appearance are separated by some matrix material. Hematite has a whitish-grey coloration and is distinguished from goethite by the intense and bright reddish-brown coloration of goethite (Fig. 5c). Goethite appears to replace hematite (Fig. 5c), corroborating the observation under transmitted light that the oxidation of hematite led to the formation of goethite.

Pyrite is found to occur close to and in association with hematite and shattered quartz (Fig. 5d). This may imply that pyrite was emplaced by hydrothermal fluids after the shearing of the quartz veins in the Kunche area, before lateritization. Sphalerite is found within hematite as a subhedral crystal and blebs and as selvages along the boundaries of deformed hematite (Fig. 5e). Goethite and recrystallized quartz occur within masses of hematite and within these same masses of hematite are late phase sphalerite blebs (Fig. 5f).

Pyrite oxidized to hematite while goethite was produced by the hydration and oxidation of hematite (Fig. 5f).

Sulphide-bearing minerals such as pyrite (FeS_2), associated with the mineralization in the area were precipitated under favorable conditions from the hydrothermal fluids that pervaded the host rocks within the Wa-Lawra Belt (Amponsah *et al.*, 2015). The weathering of quartz veins released both Fe and S into the laterites. Sphalerite (ZnS) was formed by similar processes, but not the same event responsible for Au-rich quartz veins in the area as suggested by the correlation analysis. Thus, Zn within laterites was emplaced by the breakdown of sphalerite. This is supported by the findings of Langman and Moberly (2018) that the weathering of sphalerite releases Zn into the geochemical environment. Therefore, it can be inferred that Pb, As, and Cu contents within the residual laterites are in part due to the presence of galena (PbS), arsenopyrite (AsFeS), and chalcopyrite ($CuFeS_2$), which have been reported in the Wa-Lawra Belt (Amponsah *et al.*, 2015).

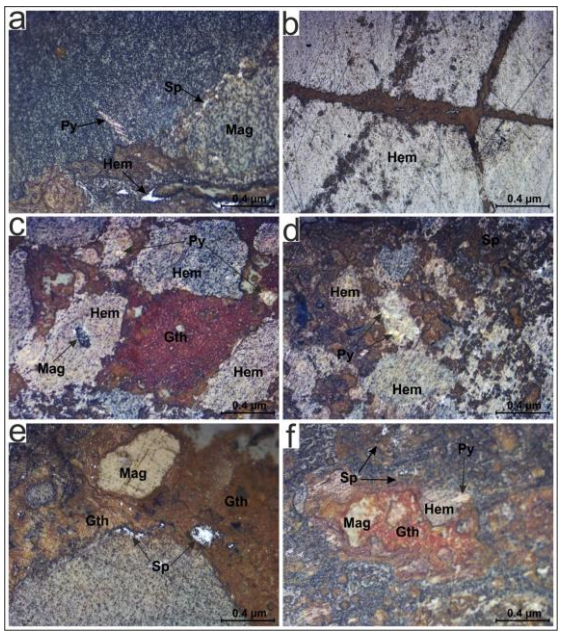

Figure 5. Photomicrograph Images of the Studied Samples (Qtz = Quartz, Py = Pyrite, Hem = Hematite, Sp = Sphalerite, Mag = Magnetite, Gth = Goethite)

3.2 Multi-element geochemistry

The multi-element geochemistry of the residual laterite samples from the Kunche area is summarized in Table 1 where the mean concentrations and range (minimum and maximum) of concentrations for the elements of most interest are respectively given as follows: 32.1 % and 8.27-46.1 wt. % for Fe; 0.36 % and 0.19-0.49 wt. % for S; 734 ppm and 215-1439 ppm for Mn, 32.4 ppm and 0.00-155 ppm for Ni, 77.5 ppm and 14.0-411 ppm for Cu, 42.3 ppm and 6.00-71.0 ppm for Pb, 75.9 ppm and 0.00-147 ppm for As, 5.50 ppm and 0.02-62.0 ppm for Ag, 95.7 ppb and 18.0-196 ppb for Au and 19.1 ppm and 0.00-90.0 ppm for Zn.

Table 1. Summary statistics of untransformed element concentrations obtained from residual laterite samples in the Kunche area (concentrations of Fe and S are in %, Au in ppb, and the rest in ppm)

Element	Min	Max	Mean	STD	Variance
Fe	8.27	46.1	32.1	11.3	127
S	0.19	0.49	0.36	0.09	0.01
Mn	215	1439	734	363	131931
Ca	514	2507	1077	549	301382
Ti	1259	3167	2081	597	356868
Cr	291	1027	554	236	55677
Ni	0.00	155	32.4	46.1	2123
Co	0.00	1794	750	601	361399
Cu	14.0	411	77.5	109	11903
Rb	11.7	42.9	24.3	8.12	66.0
Sr	5.10	39.8	15.4	11.3	127
Zr	47.0	282	159	73.3	5366
Y	0.00	12.5	5.85	3.80	14.5
Pb	6.00	71.0	42.3	20.5	419
Zn	0.00	90.0	19.1	27.9	778
As	0.00	147	75.9	55.1	3037
Au	18.0	196	95.7	56.4	3177
Ag	0.02	62.0	5.50	17.8	317

In a box and whisker plot which involves Fe, S, Pb, Mn, Ni, As, Cu, Zn, Au, and Ag, Mn is observed as the most dominant element in the residual laterites

since its whisker lies well above that of all other elements (Fig. 6). Sulfur has the least dominance due to its extremely small box and whisker relative to the other elements (Fig. 6). This may imply that the laterites were derived from the basic Birimian metavolcanic rocks underlying them.

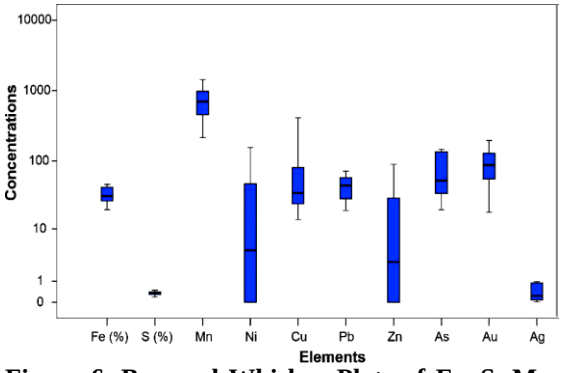

Figure 6. Box and Whisker Plots of Fe, S, Mn, Ni, Cu, Pb, Zn, As, Au, and Ag (Fe and S in wt. %, Au in ppb, and the rest in ppm)

3.3 Statistical analysis

3.3.1 P-P plots

P-P plots of Ag, As, Cu, and Au in Fig. 7 show deviation from the normal distribution and skewness. This is because regional geochemical data seldom shows a normal distribution. This means the raw dataset arises from more than one association of elements, and this can be linked to different geochemical processes (Zuo, 2011).

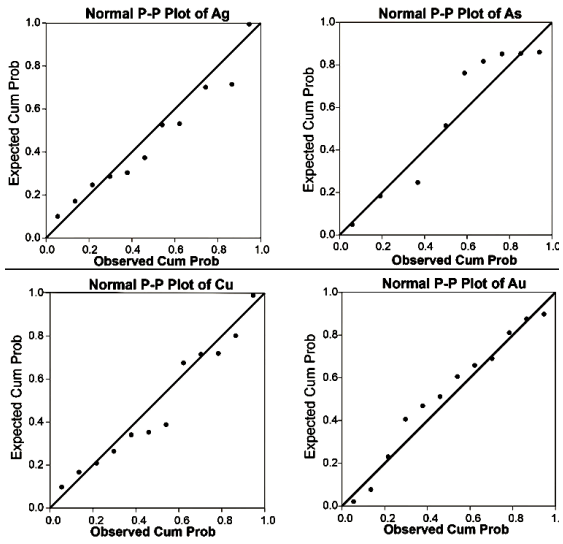

Figure 7. P-P Plots for Ag, As, Cu, and Au

3.3.2 Correlation analysis

Spearman's correlation revealed a strong positive correlation between Fe and S (r = 0.84), Mn and Rb (r = 0.76), Zr and Ti (r = 0.81), Pb and Fe (r = 0.86), Pb and S (r = 0.75), S and Au (r = 0.71), as well as Ag and Au (r = 0.80) (Table 2). Moderate positive correlation exists between Fe and Cr (r = 0.66), S and Cr (r = 0.56), Mn and Cu (r = 0.65), Rb and Cu (r = 0.51), Zr and Sr (r = 0.55), Zn and As (r = 0.57), Cu and Au (r = 0.57), as well as S and Ag (r = 0.51) (Table 2).

Strong to moderate negative correlation is seen to occur between Mn and Ni (r = -0.59), Ca and Ni (r = -0.61), Fe and Rb (r = -0.53), Ni and Rb (r = -0.59), Cr and Sr (r = -0.55), Ni and Sr (r = -0.58), Mn and Zr (r = -0.56), Cu and Zr (r = -0.55), Ca and Zn (r = -0.76), as well as Ca and As (r = -0.71) (Table 2). For the elements of interest, Au shows strong positive correlation with Ag (r = 0.80) and S (r = 0.71), and moderate positive correlation with Cu (r = 0.57) (Table 2). For the remaining selected elements, Au correlates weakly and positively with Fe (r = 0.37), Pb (r = 0.34), and As (r = 0.46) (Table 2). The occurrence of Au and Zn is likely to be a result of different geochemical processes since the correlation between Au and Zn is negatively negligible with r = -0.02 (Table 2).

3.3.3 Factor analysis

83.29 % of the total variance is defined by 5 factors with eigenvalues greater than 1. Factor 1 accounts for 26.52 % of the total variance and represents Pb-Co-Fe-S multi-element associations (Fig. 8). Elements within this factor result from two sources. Fe, Pb, and S are from sulfide ore minerals and were enriched by the hydromorphic processes. Fe and S in any factor represent the dominance of Fe-oxides. Cobalt on the other hand results from mafic host rocks in the area (lithogenic effect) (Helba *et al.*, 2020). Thus, this factor shows both hydromorphic dispersion and lithogenic control.

Factor 2 accounts for 20.35 % of the total variance and represents Rb-Mn-Cu-Au multi-element associations (Fig. 8). Au and Cu were deposited by hydrothermal solutions that circulated in the wall rocks. Mn and Rb are from wall rocks. Thus, this factor indicates hydrothermal solution and wall rock inputs.

Table 2. Two-Tailed Spearman Correlation Matrix of Elements with r ≤ - 0.5 and r ≥ 0.5 Boldened

	Fe	S	Mn	Ca	Ti	Cr	Ni	Co	Cu	Rb	Sr	Zr	Y	Pb	Zn	As	Au	Ag
Fe	1.00																	
S	**0.84**	1.00																
Mn	-0.07	0.12	1.00															
Ca	0.13	0.06	0.36	1.00														
Ti	-0.22	0.03	-0.36	-0.08	1.00													
Cr	**0.66**	**0.56**	-0.01	0.01	-0.37	1.00												
Ni	0.34	0.32	**-0.59**	**-0.61**	0.14	0.41	1.00											
Co	0.14	0.20	0.21	0.01	0.14	-0.22	0.24	1.00										
Cu	0.10	0.30	**0.65**	0.06	-0.49	0.04	-0.30	-0.01	1.00									
Rb	**-0.53**	-0.30	**0.76**	0.27	-0.08	-0.48	**-0.59**	0.18	**0.51**	1.00								
Sr	-0.36	-0.39	0.13	0.34	0.28	**-0.55**	**-0.58**	0.05	0.08	0.41	1.00							
Zr	-0.20	-0.19	**-0.56**	-0.15	**0.81**	-0.36	0.13	0.07	**-0.55**	-0.21	**0.55**	1.00						
Y	-0.26	-0.41	0.18	0.07	-0.34	-0.35	-0.19	-0.06	0.25	0.36	0.00	-0.33	1.00					
Pb	**0.86**	**0.75**	0.26	0.18	-0.16	0.40	0.01	0.23	0.30	-0.18	-0.02	-0.12	-0.13	1.00				
Zn	-0.18	-0.22	-0.19	**-0.76**	-0.06	-0.08	0.40	-0.19	-0.01	-0.01	-0.33	-0.07	0.41	-0.15	1.00			
As	0.04	0.27	-0.18	**-0.71**	-0.02	-0.05	0.46	-0.05	0.43	-0.02	-0.35	-0.10	0.05	-0.04	**0.57**	1.00		
Au	0.37	**0.71**	0.34	-0.14	-0.02	0.47	0.38	0.28	**0.57**	0.12	-0.31	-0.27	-0.26	0.34	-0.02	0.46	1.00	
Ag	0.11	**0.51**	0.25	-0.07	0.04	0.47	0.19	-0.19	0.47	0.07	-0.38	-0.27	-0.22	0.01	-0.09	0.40	**0.80**	1.00

Factor 3 explains 13.54% of the total variance and represents Ag-Ni-Y multi-element associations (Fig. 8). Ag is from hydrothermal fluids while Ni and Y are from wall rocks, respectively similar to factors 4 and 1 for the untransformed dataset. Similar to the findings of Sunkari *et al*. (2019), this factor shows input from wall rocks and hydrothermal fluids as a result.

Factor 4 explains 12.78% of the total variance and represents Sr-Ti-Cr-Zr multi-element associations (Fig. 8). Elements Sr, Ti, and Zr were input from detrital material, similar to the findings of Micó *et al*. (2006). Cr is due to a lithogenic effect. Thus, factor 5 indicates the lithogenic effect and detrital material input. Factor 5 explains 10.11% of the total variance and represents As-Ca-Zn multi-element associations (Fig. 8). Ca was input by wall rocks (Ca-rich rock-forming minerals while As and Zn were input by hydrothermal sources similar to the findings of Deng *et al*. (2010). Due to the presence of Zn in this factor, sphalerite can be inferred to occur in the area.

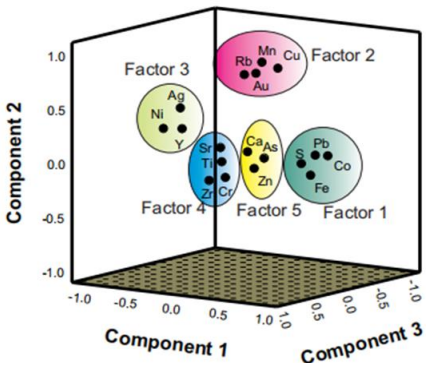

Figure 8. Factor Analysis Plot Rotated in Space

3.3.4 Hierarchical cluster analysis

Three clusters representing multi-element associations could be observed in the dendrogram derived from the transformed dataset (Fig. 11). Cluster 1 has multi-element associations of Au, Fe, S, Ag, Pb, Mn, Cr, Co, Ni, and Cu (Fig. 11).

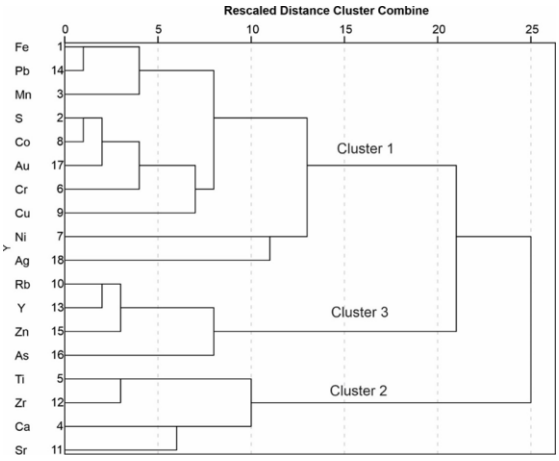

Figure 11. Dendrogram indicating Three Multi-Element Clusters

From this, As, Fe, Pb, and S are from ore minerals such as pyrite, arsenopyrite, and galena while Au and Ag are from hydrothermal fluids that pervaded host rocks while Cr is due to lithogenic control, as observed in factor analysis. Cluster 2 has multi-element associations of Ti, Zr, Sr, and Ca (Fig. 11). Elements within this cluster may be derived from wall rocks (host rocks) and transported material as inferred from factor analysis. Cluster 3 has multi-element associations of Rb, As, Y, and Zn (Fig. 11). While Rb and Y are input by lithogenic control, As and Zn are input by two different hydrothermal evens, as suggested by correlation analysis.

3.3.5 Single element geochemical anomaly mapping

Areas with anomalous single element concentrations are shown in Figures 12 and 13. Blue to light blue areas have low elemental concentrations while yellow to deep red portions are areas with significant single element geochemical anomalies. The gold anomaly map shows areas of anomalous Au contents (Fig. 12). Notable abnormal enrichment of Au can be observed in the northern parts of the area (close to the Kunche gold prospect) and southwestern parts of the area. Anomaly maps for Ag, As, Cu, and Pb are presented in Fig. 13 (a-d). Ag anomaly map of the study area shows that geochemical anomalies are mostly restricted to the northern (close to the gold prospect), central, and the south-eastern parts of the study area (Fig. 13a). Similar distributions are seen in As, Cu, and Pb maps (Fig. 13b-d).

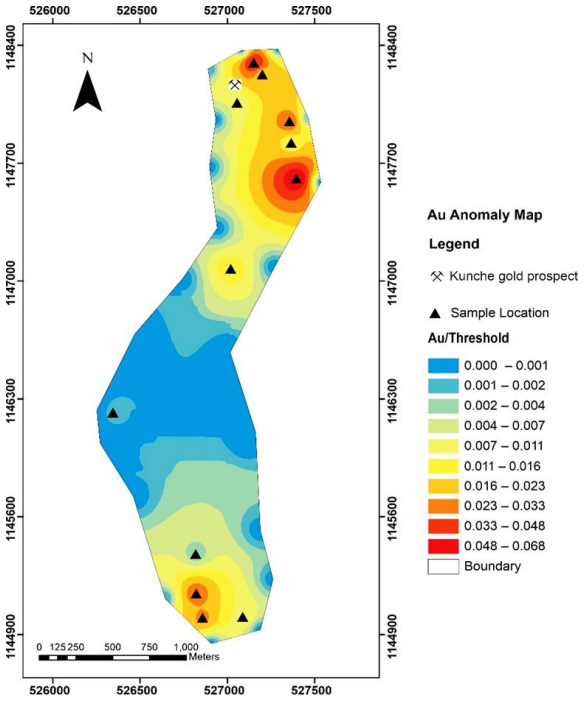

Figure 12. Single Element Anomaly Map for Au

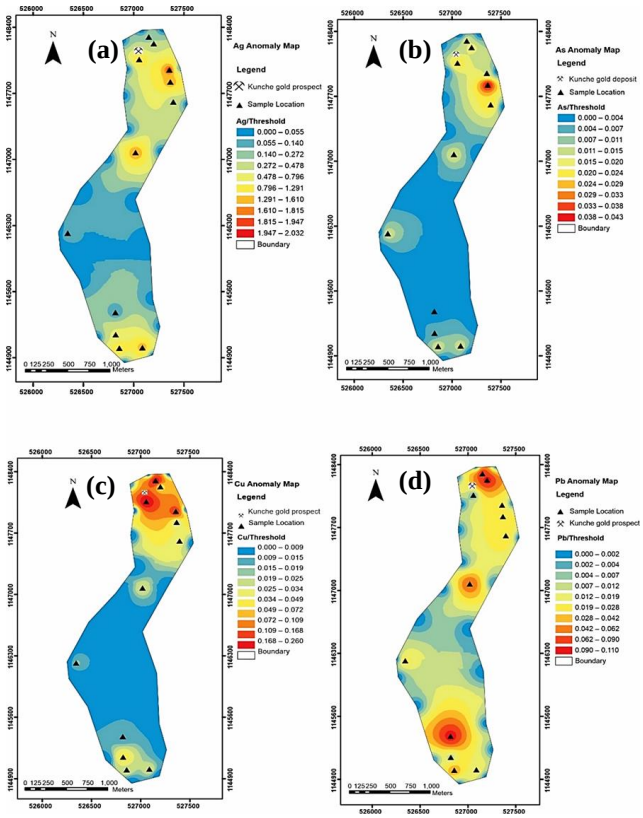

Figure 13. Single Element Anomaly Maps for (a) Ag, (b) As, (c) Cu, and (d) Pb

3.3.6 Multi-element geochemical anomaly mapping

Using the computed thresholds, geochemical halos, characterized by the existence of elevated contents of pathfinder elements related to Au mineralization were defined by applying the multi-element halo technique. Four multi-element anomaly maps were produced (Fig. 14a-d). Two of these were produced in consideration of Fe and S because of the presence of iron-sulfide ore minerals such as pyrite and the strong positive correlation that exists between Fe and S (Fig. 14a-b). Similar geochemical anomaly patterns are observed with reference to single anomaly maps.

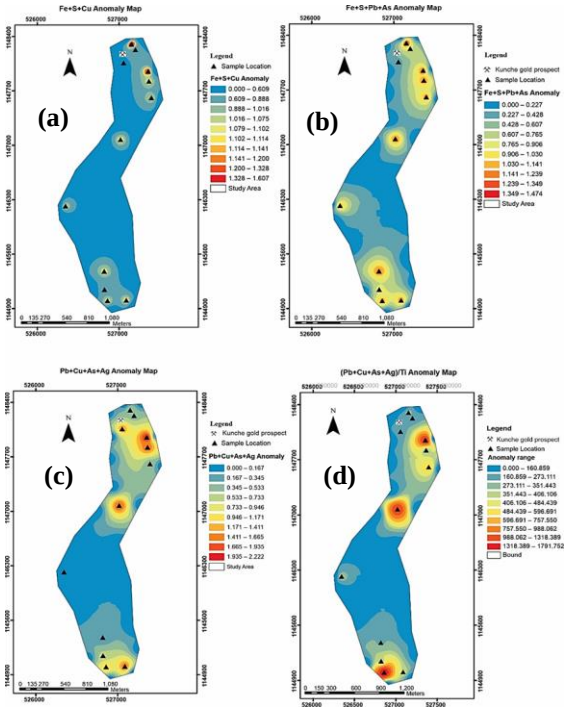

Figure 14. Multi-Element Anomaly Maps for (a) Fe+S+Cu, (b) Fe+S+Pb+As, (c) Pb+Cu+As+Ag and (d) (Pb+Cu+As+Ag)/Ti.

3.3.7 Univariate outliers and element paragenetic occurrence

The presence of several groups or populations is made evident by the occurrence of little distortions or changes in slope concentrations of Cu, Ag, Au, and As as seen in the P-P plots (Fig. 7). There are also extreme concentration values from certain samples, which seem to be detached from the rest of the dataset. They are separated from the continuous concentration distribution of the elements in the P-P plots. Samples for which certain elemental concentrations do not follow the normal distribution are indicative of outliers (Sunkari *et al*., 2019). In exploration geochemistry, outliers are most probably the evidence of anomalies related to mineralization (Filzmoser *et al.*, 2005). These outliers are also representative of different geochemical processes, as stated earlier.

A good-strong positive correlation between elements shows the paragenetic occurrence of the elements involved (Lapworth *et al*., 2012). Sunkari *et al*. (2019) revealed that such a correlation is indicative of similar geochemical processes which led to the distribution of the elements in the area. Their enrichment is therefore due to similar processes. Therefore, the good-strong positive correlation between Fe and Cr, S and Cr, Mn and Cu, Rb and Cu, Zr and Sr, Zn and As, Cu and Au, S and Ag, Fe and S, Mn and Rb, Zr and Ti, Pb and Fe, Pb and S, S and Au, as well as Ag and Au (Table 2) indicate the paragenetic occurrence of these elements. It is interpreted that similar regolith geochemical processes in the study area account for the dispersion and mobilization of these elements in the residual laterites.

However, Simmonds *et al*. (2017) mentioned that a moderate to strong negative correlation is indicative of non-paragenetic occurrence. This means that the moderate to strong negative correlations between Mn and Ni, Ca and Ni, Fe and Rb, Ni and Rb, Cr and Sr, Ni and Sr, Mn and Zr, Cu and Zr, Ca and Zn, as well as Ca and As (Table 2) were due to different regolith geochemical processes together with dispersion and concentration of elements by leaching of elements during events of lateritization and dilution or enrichment of elements during intermixing of surface or groundwater in the area.

Also, the strong positive correlation between Au and Ag, Cu, and S is directly related to the occurrence of gold in the area. Au correlates weakly and positively with Fe, Pb, and As (Table 2), implying that Fe, Pb, and As could have occurred with Au, however, they were subsequently redistributed by multiple regolith geochemical processes (Sunkari *et al*., 2019). The negative negligible correlation between Au and Zn is probably due to complex regolith geochemical processes.

3.2.3 Identification of pathfinder elements from multivariate statistical analyses

From the factor analysis, the transformed dataset reveals that factor 1 with element associations involving Fe-S-Co-Pb and factor 2 with element associations of Mn-Cu-Rb-Au are similar to cluster 1 from the HCA with multi-element associations of Au, Fe, S, Ag, Pb, Mn, Cr, Co, Ni, and Cu. This similarity confirms the inferred sulfide ore minerals, mafic host rocks, wall rocks, and hydrothermal fluid inputs (Sunkari et al., 2019; Fagbohun *et al.*, 2021; Mvile *et al.*, 2021). Factor 4 from the factor analysis with element associations of Ti-Cr-Sr-Zr is similar to cluster 2 from the HCA with element associations of Ti-Sr-Zr-Ca. This similarity also confirms the detrital material and wall rock inputs of the elements involved. Cluster 3 from HCA with element associations of Zn-As-Y-Rb is similar to factor 5 from the factor analysis with element associations of Zn-As-Ca. This similarity also further validates the hydrothermal solution and wall rocks input of the elements involved (Fagbohun *et al.*, 2021). Considering all these, using cluster 1 of the transformed data from the HCA is the best element grouping followed by cluster 3 when identifying pathfinder elements of gold in the area. From this, Cu, Pb, Ag, and As may be regarded as the elemental cluster related to the occurrence of gold in the Kunche area. As stated from the correlation analysis, there is a positive correlation between Cu, Pb, Ag, As, and Au. Zn is on the other hand unrelated to Au occurrence in the area due to its negative negligible correlation with Au (r = -0.02). Therefore, Cu, Pb, Ag, and As can be identified as the pathfinders of Au in the area.

4 Conclusions

This study focused on only residual laterites obtained from areas where the land surface is elevated such as hills, ridges, and plateaus in the study area. Petrographic studies reveal amphibole, clinopyroxene, quartz, magnetite, hematite, goethite, pyrite, and sphalerite. Box and Whisker Plots show Mn and S as the most dominant and least dominant elements within the residual laterites in the area, respectively. P-P plots reveal that the multi-element geochemical data obtained from these laterites stemmed from more than one population as a result of different geological processes, made evident by kinks in the slopes of the plots for selected elements. Spearman's correlation, factor analysis, and hierarchical cluster analysis identified Pb, Cu, Ag, and As to be directly related to the occurrence of Au in the Kunche area.

Pb, Cu, Ag, and As can be therefore considered as the elemental cluster related to the occurrence of Au in the Kunche area. This implies that Cu, Pb, Ag, and As are the indicator elements of gold in the Wa-Lawra Belt. This finding is not different from those of earlier studies, where soil/laterites from mixed sources were used. Therefore, using residual laterites as well as laterites from mixed sources will likely produce similar results concerning pathfinder elements in the Wa-Lawra Belt.

Acknowledgments

This study is part of the Bachelor thesis of the second author at the University of Mines and Technology, Tarkwa, Ghana. The authors wish to thank Azumah Resources Limited, Ghana for their immense contribution to the acquisition of the samples and data used for this study. Special thanks also go to the Petrology Laboratory Technician of the University of Mines and Technology, Tarkwa, Ghana, Mr Abdul-Rahman Abdullah, for his relentless support during the preparation of the thin and polished sections.

References

Akintola, A. I., Olorunfemi, A. O., Bankole, S. I., Omotoye, S. J. and Ajayi, B. O. (2013), "Petrography and Geochemical evaluation of major and trace element concentrations in the stream sediments of Itagunmodi and its environs, Southwestern, Nigeria", *Journal of Earth Sciences and Geotechnical Engineering* Vol. 3, No. 4, pp 1-24.

Amponsah, P. O., Salvi, S., Béziat, D., Siebenaller, L., Baratoux, L. and Jessell, M. W. (2015), "Geology and Geochemistry of the Shear Hosted Julie Deposit, NW Ghana", *Journal of African Earth Sciences*, Vol. 112, pp. 505-523.

Arhin, E. (2013), "Use of Regolith Geochemistry to Delineate Gold Mineralization under cover: a case study in the Lawra Belt, NW Ghana", *Unpublished Ph.D. Thesis*, Department of Geology, University of Leicester, UK, 286 pp.

Arhin, E., Jenkin, G. R., Cunningham, D. and Nude, P. (2015), "Regolith mapping of deeply weathered terrain in savannah regions of the Birimian Lawra Greenstone Belt, Ghana", *Journal of Geochemical Exploration*, Vol. 159, pp. 194-207.

Arhin, E. and Nude, P. (2009), "Significance of Regolith Mapping and Its Implication for Gold Exploration in Northern Ghana: A Case Study at Tinga and Kunche", *Geochemistry: Exploration, Environment and Analysis*, Vol. 9, pp. 63-69.

Debrah, T. (2013), "Identifying Pathfinder Elements for Gold in A Multi-Element Soil Geochemical Data, Owere Mines Limited, Konongo" *Unpublished BSc. Project Work*, University of Mines and Technology, pp. 3-20.

Deng, J., Wang, Q., Yang, L., Wang, Y., Gong, Q. and Liu, H. (2010), "Delineation and explanation of geochemical anomalies using fractal models in the Heqing area, Yunnan Province, China", *Journal of Geochemical Exploration*, Vol. 105, No. 3, pp. 95-105.

Fagbohun, B. J., Bamisaiye, O. A., Ayoola, F. J., Omitogun, A. A. and Adeoti, B. (2021), "Identifying geochemical anomalies and spatial distribution of gold and associated elements in the Zuru Schist Belt, northwest Nigeria", *Arabian Journal of Geosciences*, Vol. 14, No. 6, pp. 1-20.

Filzmoser, P., Garrett, R. G. and Reimann, C. (2005), "Multivariate outlier detection in exploration geochemistry", *Computers & Geosciences*, Vol. 31, Vol. 5, pp. 579-587.

Gao, Y. and Chik, A. B. R. (2013), "A Multiple Regression Analysis on Influencing Factors of Urban Services Growth in China", *Technology and Investment*, Vol. 4, pp. 1-5.

Griffis, J., Barning, K., Agezo, F.L. and Akosa, F. (2002), *Gold deposits of Ghana*, Mineral Commission, Accra, Ghana, 432 pp.

Helba, H. A., Khalil, K. I., Mamdouh, M. M. and Khalek, I. A.A. (2020), "Zonation in primary geochemical haloes for orogenic vein-type gold mineralization in the Quartz Ridge prospect, Sukari gold mine area, Eastern Desert of Egypt", *Journal of Geochemical Exploration*, Vol. 209, 106378 pp.

Langman, J. B. and Moberly, J. G. (2018), "Weathering of a mined quartz-carbonate, galena-sphalerite ore and release and transport of nanophase zinc carbonate in circumneutral drainage", *Journal of Geochemical Exploration*, Vol. 188, pp. 185-193.

Lapworth, D. J., Knights, K. V., Key, R. M., Johnson, C. C., Ayoade, E., Adekanmi, M. A., Arisekola, T. M., Okunlola, O. A., Backman, B., Eklund, M. and Everett, P.A. (2012), "Geochemical mapping using stream sediments in west-central Nigeria: Implications for environmental studies and mineral exploration in West Africa", *Applied Geochemistry*, Vol. 27, No. 6, pp. 1035-1052.

Micó, C., Peris, M., Recatala, L. and Sanchez, J. (2006), "Assessing heavy metal sources in agricultural soils of a European Mediterranean area by multivariate analysis", *Chemosphere*, Vol. 65, No. 5, pp. 863-872.

Mvile, B. N., Abu, M. and Kalimenze, J. (2021), "Trace Elements Geochemistry of In Situ Regolith Materials and Their Implication on Gold Mineralization and Exploration Targeting, Dodoma Region, East Africa", *Mining, Metallurgy & Exploration*, Vol. 38, No. 5, pp. 2075-2087.

Nude, P. M., Asigri, J. M., Yidana, S. M., Arhin, E., Foli, G. and Kutu, J.M. (2012), "Identifying Pathfinder Elements for Gold in Multi-Element Soil Geochemical Data from the Wa-Lawra Belt, Northwest Ghana: A Multivariate Statistical Approach", *International Journal of Geosciences*, Vol. 3, No. 1, pp. 62-70.

Reid, A. (2009), "The Olympic Cu-Au Province, Gawler Craton: Review of the Lithospheric Architecture, Geodynamic Setting, Alteration Systems, Cover Successions, and Prospectivity". *Minerals*, Vol. 9, No. 6, 371 pp.

Reimann, C., Filzmoser, P. and Garrett, R.G. (2005), "Background and threshold: a critical comparison of methods of determination", *Science of the Total Environment*, Vol. 346, No. 1-3, pp. 1-16.

Reis, A. P., Sousa, A. J. and Fonseca, E.C. (2001), "Soil Geochemical Prospecting for Gold at Marrancos (Northern Portugal)", *Journal of Geochemical Exploration*, Vol. 73, No. 1, pp. 1-10.

Simmonds, V., Jahangiryar, F., Moazzen, M. and Ravaghi, A. (2017), "Distribution of base metals and the related elements in the stream-sediments around the Ahar area (NW Iran) and their implications", *Chemie der Erde – Geochemistry*, Vol. 77, No. 3, pp. 429-441.

Sunkari, E. D. Abu, M., Zango, M. S. and Wani, A. M. L. (2020), "Hydrogeochemical characterization and assessment of groundwater quality in the Kwahu-Bombouaka Group of the Voltaian Supergroup, Ghana", *Journal of African Earth Sciences*, Vol. 169, 103899 pp.

Sunkari, E. D., Appiah-Twum, M. and Lermi, A. (2019), "Spatial distribution and trace element geochemistry of laterites in Kunche area: Implication for gold exploration targets in NW, Ghana", *Journal of Africa Earth Sciences*, Vol. 158, 103519 pp.

Sunkari, E. D. and Zango, M. S. (2018), "Preliminary investigation of the geologic controls of graphite mineralization and exploration potential of the Wa-Lawra Belt: Implications for Kambale graphite deposit", *J. Environ. Earth Sci*, Vol. 8, No. 3, pp. 77-89.

Waller, C., Franey, N., Hodgson, S. and Widenbar, L. (2012), *NI-43-101 Technical Report for Azumah Resources LTD*, Wa Gold Project, Ghana, 114 pp.

Zhao, J., Chen, S. and Zuo, R. (2015), "Identifying geochemical anomalies associated with Au – Cu mineralization using multifractal and artificial neural network models in the Ningqiang district, Shaanxi, China", *Journal of Geochemical Exploration*, Vol. 164, pp. 54-64.

Zuo, R. (2011), "Identifying geochemical anomalies associated with Cu and Pb–Zn skarn mineralization using principal component analysis and spectrum–area fractal modeling in the Gangdese Belt, Tibet (China)", *Journal of Geochemical Exploration*, Vol. 111, Vol. 1-2, pp. 13-22.

Authors

Emmanuel Daanoba Sunkari is a Technical Instructor at the University of Mines and Technology, Tarkwa. He is currently a Ph.D. Scholar at Niğde Ömer Halisdemir University, Turkey. He obtained an MSc in Geological Engineering from Muğla Sitki Koçman University, Turkey, and holds a BSc in Earth Science from the University for Development Studies, Ghana. His research aims to contribute significantly to our understanding of the petrology and genesis of hydrothermal ore deposits, groundwater evolution, and sources of contaminants in environmental media within mining and post-mining areas.

Samuel Edem Kodzo Tetteh is a Research and Teaching Assistant at the University of Mines and Technology. He holds a BSc in Geological Engineering from the University of Mines and Technology, Tarkwa, Ghana. He is a student member of the West African Institute of Mining, Metallurgy and Petroleum (WAIMM) and an associate member of the Ghana Institute of Geoscientists (GhIG). His research interests include economic geology, petrology, and geochemistry.

Moses Sumbobo is an Exploration Geologist at Azumah Resources Limited, Nadowli, Ghana and holds a Bachelor of Science degree in Earth Science from the University for Development Studies, Ghana. His research interests are in petrology and exploration geochemistry.

Yilmaz Demir is an Associate Professor at the Department of Geological Engineering, Recep Tayyip Erdoğan University, Turkey. His researches generally focus on the genesis of ore deposits using multidisciplinary approaches such as geochemistry, fluid inclusion studies, and stable isotopic studies.